High efficiency Yb:YAG crystalline fiber-waveguide lasers

Xiaodong Mu,[1,*] Stephanie Meissner,[1] Helmuth Meissner,[1] and Anthony W. Yu[2]

[1]*Onyx Optics, Inc., 6551 Sierra Lane, Dublin, California 94568, USA*

[2]*NASA Goddard Space Flight Center, Greenbelt, Maryland 20771, USA*

**Corresponding author: xmu@onyxoptics.com*

Received August 12, 2014; revised October 1, 2014; accepted October 10, 2014;
posted October 10, 2014 (Doc. ID 220863); published October 30, 2014

A laser diode (LD) cladding pumped single-mode 1030 nm laser has been demonstrated, in an adhesive-free bonded 40 μm core Yb:YAG crystalline fiber waveguide (CFW). A laser output power of 13.2 W at a wavelength of 1.03 μm has been achieved, for an input pump power of 39.5 W. The corresponded laser efficiency is 33.4%. The laser beam quality is confirmed to be near diffraction-limited, with a measured $M^2 = 1.02$. A LD core pumped single-clad Yb:YAG CFW laser has also been demonstrated with a top-hat laser beam profile, with a laser output power of 28 W and a slope efficiency of 78%. © 2014 Optical Society of America

OCIS codes: (140.3510) Lasers, fiber; (140.3280) Laser amplifiers; (230.7380) Waveguides, channeled.
http://dx.doi.org/10.1364/OL.39.006331

Rare-earth (RE) doped YAG crystalline fibers have the potential for tens of kilowatts of laser output power, due to their much higher thermal conductivity and lower stimulated Brillouin scattering (SBS) threshold, compared with conventional glass fibers [1]. Although current fiber growth (or pulling) techniques, such as laser heated pedestal growth (LHPG) [2–4] and micro pulling down [5,6], have made impressive advances on producing a low loss single-crystal fiber core, they have not yet been successful in producing double-clad, or even single-clad, fully crystalline fibers with controlled differences in refractive indices. In order to circumvent the problems in the fabrication of crystalline fibers, and still fully utilize the advantages of crystal fibers over glass fibers, we have realized a method for producing true crystalline fiber waveguides (CFWs) from YAG and other crystalline materials, by employing Onyx Optics' adhesive-free bond (AFB) technology. The method has been successfully used for producing low optical loss single-mode YAG waveguides, with a variety of RE dopants [7,8]. A recent laser experiment has further demonstrated a nearly quantum defect limited efficiency in a single-clad 1.6-μm Er:YAG CFW laser, that was in-band pumped by another fiber laser at 1.532 μm [8]. In addition, a laser power of over 400 W has been also demonstrated in a Yb:YAG planar waveguide recently [9], which demonstrates the high power scalability of the waveguides made by the adhesive-free bonding technology. In this Letter, we report the first laser diode (LD) cladding pumped single-mode 1030 nm laser in a double-clad 40-μm core Yb:YAG CFW, with a near diffraction-limited beam quality of $M^2 = 1.02$. The laser output power is 8.5 W with uncoated bare waveguide ends, and is 13.2 W with attached laser mirrors, for a pump power of 39.5 W. The optical to optical efficiencies in the two setups are 21.5 and 33.4%, respectively. We have also demonstrated a LD pumped laser in a single-clad Yb:YAG CFW. A maximum output power of 28 W and a slope efficiency of 78% have been achieved.

The double-clad CFW used in the experiment consists of a 1 at. % Yb:YAG square waveguide core with un-doped YAG inner cladding, and ceramic spinel outer cladding as shown in Fig. 1(a). It was made from a single-crystal Yb:YAG slab followed by multiple precision polishing and crystal bonding processes, for the final core size as well as the formation of the inner and outer claddings. The measured cross sections for the waveguide core and the inner cladding are around 40×40 μm and 102×102 μm, respectively. In order to simplify the fabrication process and also increase the cooling efficiency, the outer cladding is only bonded on three sides of the inner cladding, so that the un-clad side [the lower side of Fig. 1(a)] can directly contact with a heat sink. The outer cladding cross section is 4.3×6.4 mm and the waveguide length is 65 mm. The calculated numerical apertures (NAs) of the waveguide core and the inner cladding are around 0.02 and 0.63, respectively. In the calculation, we use $n(\text{spinel}) = 1.703$ and $n(\text{YAG}) = 1.816$ for a wavelength around 1 μm [10,11]. The refractive index step between the 1 at. % Yb:YAG and the YAG inner cladding is considered to be small, and also sensitive to the accuracy of the doping concentration, as well as different crystal suppliers. In the research reported in this Letter, we have directly measured the refractive index difference between the two crystals in a pre-bonded Yb:YAG/YAG doublet, with an interferometer at a wavelength of 1.55 μm [7,12]. The refractive index increase is found to be $\Delta n = 1.08 \times 10^{-4}$ for the 1 at. % Yb:YAG used in the research reported in this Letter, which corresponds to a NA = 0.02 for the waveguide core. The second CFW used in the experiment is a single-clad waveguide as shown in

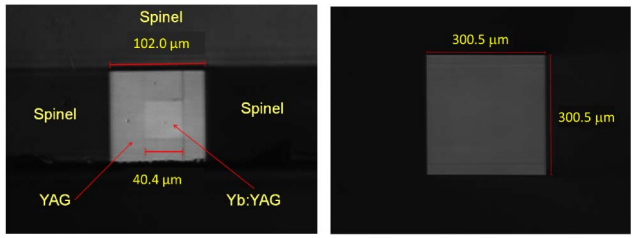

(a) (b)

Fig. 1. Microscope end images: (a) double-clad Yb:YAG CFW; and (b) single-clad Yb:YAG CFW.

 © 2014 Optical Society of America

Fig. 1(b). It consists of a 0.3 at. % Yb:YAG waveguide core of a cross section of 300×300 μm. The outer cladding is ceramic spinel so that a large NA ($= 0.63$) can be formed for direct LD core pumping. The waveguide length is 100 mm.

In general, the adhesive-free bonded RE-doped YAG CFW can be considered as having a near-perfect step-index profile. This is due to the stable lattice structure of the YAG crystal, in which the trivalent RE ions substitute for Y^{3+} at the lattice position that is surrounded by eight oxygen ions [13]. Therefore, ion diffusion from the RE-doped YAG core to the un-doped YAG is not expected to happen in our bonding processes. The waveguide mode in this type of square core dielectric waveguide has been numerically solved by finite-element analysis and other approaches [14–16]. According to those calculations, a single-mode waveguide can be achieved when a parameter $B < 1.37$ with $B = 2d \cdot \mathrm{NA}/\lambda$, where d is the square core width. Based on this criterion, the double-clad CFW used in the research reported in this Letter will have two propagation modes. The single clad waveguide will be a multimode waveguide with over hundreds of modes.

The laser experimental setup is schematically illustrated in Fig. 2. The CFW is wrapped with indium foil and clamped on a water-cooled copper heat sink, with the coolant temperature setting at 12°C. The pump laser is a fiber coupled LD that has a peak wavelength of 938 nm, and spectral line width of 5 nm. The core diameter of the delivery fiber is 150 μm and NA $= 0.22$. The pump laser is first collimated and then focused into the inner cladding from one end of the CFW, by two aspheric lenses f_1 and f_2 (both have $f = 11$ mm). A short-wave pass dichroic beam splitter (BS), with $T = 92\%$ at 940 nm and $R = 98\%$ at 1030 nm, is inserted between the two aspheric lenses at an angle of 45°, so that the pump power can be measured and the backward propagating laser beam can be extracted out for the case where the laser is operated, just with the two bare ends of the waveguide. An external laser resonator is formed by two plane mirrors that are directly attached on the two ends of the CFW with fluorinated oil. The input mirror M_1 has $T = 92\%$ at 940 nm, and $R = 99.9\%$ at 1030 nm. The output coupler (OC) M_2 has $R = 99.4\%$ at 940 nm, and a coupling efficiency of $T = 53\%$ at 1030 nm. In order to precisely measure the laser power, another OC plate is used in front of the power meter (PM), as a dichroic filter to remove the residual pump light from the 1030 nm laser output. Since the OC used in this experiment is for obtaining preliminary laser results only, it therefore may not be the optimized OC for the two CFWs.

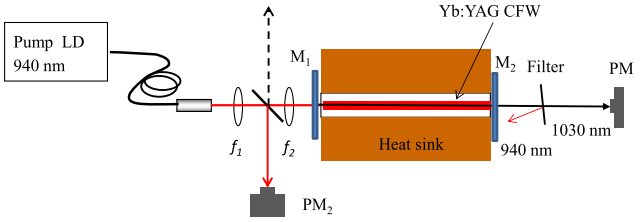

Fig. 2. Experimental layout of the cladding pumped CFW and laser output profile; f_1 and f_2, aspheric lenses.

In the experiment, we have found that when the pump power is increased to above 2.7 W, a strong laser output at 1030 nm is achieved even without the attached laser mirrors. This demonstrates that the double-clad CFW has a much larger gain coefficient ($gl > 5$) than in any bulk lasers. The laser beam in this case is coupled out by the two uncoated ends ($R \sim 8\%$) of the CFW, in both forward and backward directions, with identical output powers as shown in Fig. 3. The total laser power in the two directions is 8.5 W at an input pump power of 39.5 W, which corresponds to an optical-to-optical efficiency of 21.5%. The measured slope efficiency from Fig. 3 is 22.6%. The laser wavelength is confirmed at 1030 nm, and the spectral line width (full width at half maximum) is 4 nm with a 1/8 m monochromator (Spectral Product, CM110). After attaching the input and output laser mirrors on the two waveguide ends with fluorinated oil, the laser threshold is reduced to below 0.54 W. The maximum output power is increased to 13.2 W at a pump power of 39.5 W. Due to the low laser threshold, the laser optical to optical efficiency and the slope efficiency are almost same. They are both around 33.4%.

The near-field laser beam profile is measured in Fig. 4 by a pyroelectric camera (Spiricon Pyrocam III), at the image plane of a 10× microscope objective. The inserted image of Fig. 4 is the measured 2D beam profile. The measured roundness is about 94%, even though the waveguide core is square. The solid curve in Fig. 4 is the normalized beam intensity along one axis of the waveguide end. It is a near-perfect Gaussian distribution, with a measured beam diameter of 44 μm at the position of $1/e^2$ of the peak intensity. The beam quality is analyzed by the knife-edge method [17]. Figure 5 shows the measured beam radius as a function of the test position after a 200 mm focus lens. The fitted M^2 from Fig. 5 is ~1.02, which demonstrates that a purely single-mode laser has been achieved. The dashed curve in Fig. 4 is the calculated mode profile of the fundamental mode by Marcatili's approximation [13]. In the calculation, we use a waveguide core size $d = 40$ μm and refractive index step $\Delta n = 1.08 \times 10^{-4}$. The calculated beam diameter is 43.6 μm. One can see that the measured beam profile

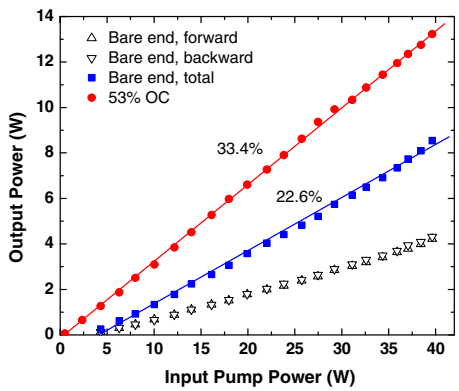

Fig. 3. Laser output power as a function of pump power. The upward and downward open triangles, and the solid squares, are the measured forward, backward, and total laser power from the uncoated CFW ends, respectively. The solid circles are the laser power after the input and output mirrors are attached.

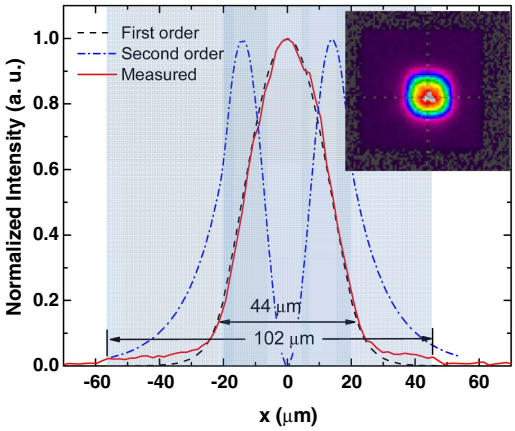

Fig. 4. Measured (solid curve) and simulated (dashed curves) beam profiles of the doubled-clad CFW laser. The dark and light shaded areas indicate the waveguide core and inner cladding, respectively. The inset shows the 2D beam profile measured by a pyroelectric camera.

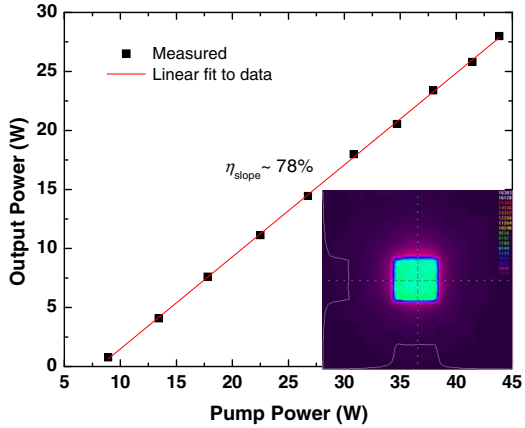

Fig. 6. Laser output power as function of pump power measured in the single-clad CFW. The inset shows the 2D beam profile measured by a pyroelectric camera.

overlaps with the calculated fundamental mode nearly perfectly, which further demonstrates that the laser output is purely single mode. It is worth mentioning that a second waveguide mode theoretically exists in this waveguide, with an effective refractive index $n_{\mathrm{eff}} = 1.81601$ (versus $n_{\mathrm{eff}} = 1.81607$ for the fundamental mode). The reason that we did not observe the second-order waveguide mode in the laser experiment can be attributed to its much weaker confinement compared with the fundamental mode, which leads to higher waveguide loss as well as a poor overlap between the second-order waveguide mode and the core, as illustrated in Fig. 4. The previously mentioned experimental result indicates that single-mode lasing is still achievable in a large mode area multimode CFW, when the waveguide only contains low-order modes. The same principle has been used in multimode glass fibers for single-mode laser operation [18].

In the single clad CFW, laser output can only be achieved with the laser mirrors attached. The laser power dependence has been measured in Fig. 6. A maximum output power of 28 W has been achieved at a pump power of 44 W. The optical-to-optical efficiency and slope efficiency are 64% and 78%, respectively. The laser beam, as indicated in the inset shown in Fig. 6, has a top-hat beam profile, with an estimated beam quality of $M_x^2 = 27$ and $M_y^2 = 12$.

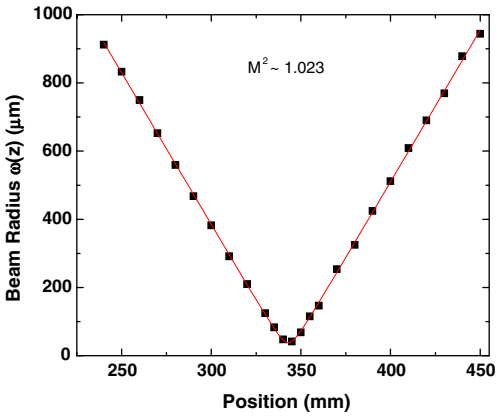

Fig. 5. Beam radius as a function of position after a 200 mm focus lens.

As the first demonstration of a LD pumped single-mode CFW laser, the laser efficiency in the research reported in this Letter is lower than the efficiencies that have been demonstrated in glass fibers [19,20]. The reason is mainly due to the nonoptimized waveguide and laser conditions. (1) Under our current pump condition, we found that the maximum laser output power only occurs when the pump spot is focused on the end of the CFW at an image ratio of 1:1 (this could be due to the small NA < 0.3 of our current lens setup and the multimode output of the delivery fiber). This means that not all the pump beam can be coupled in the waveguide inner cladding. A further analysis, based on a 2D beam profile of the pump spot captured by the pyroelectric camera at the pump end, indicates that the coupling efficiency is only about 74.6%. In this Letter, we assume that all of the pump beam inside the 100 μm inner cladding square area will be coupled into the waveguide, due to the large NA of the inner cladding. (2) The calculated pump absorption efficiency, based on the peak absorption coefficient ($\alpha \approx 1\ \mathrm{cm}^{-1}$) of the 1% at. Yb:YAG at 940 nm, is about 87.5% for the double-pass pump arrangement. However, since our pump wavelength is slightly off the peak absorption wavelength and the pump linewidth cannot be zero, the practical absorption efficiency should be less than the calculated efficiency. Based on the reflected residual pump power from the input beam splitter, the estimated pump absorption efficiency is about 78%, which is about 11% less than the calculated efficiency. (3) Due to the small NA of the waveguide core to the inner cladding, the feedback from the waveguide ends may suffer a certain feedback loss, if the waveguide end is not perfectly perpendicular to the core. The measured tilt angles for the double-clad waveguide are about 1.4' at the input end and 4' at the output end, respectively. The reflection loss in this case is estimated to be around 7% of the reflected power at the output end [21]. In addition, the small NA may also cause the waveguide modes more easily leaking to the inner cladding. Indeed, in Fig. 4 one can clearly see a certain amount of laser luminescence in the full cross section of the waveguide inner cladding.

Theoretically, an ideal Gaussian beam contains 86.4% of the total energy inside the $1/e^2$ intensity radius. This percentage of energy measured in the double-clad CFW laser is about 77.8%. The energy outside of the beam radius is increased by about 8.6%. We may attribute this energy difference to the sum of the waveguide leaking and the feedback losses at the two waveguide ends. After considering the previously mentioned losses in the pump beam and the waveguide, the actual laser efficiency in the double-clad CFW could be above 60%. One can see that this result is fairly consistent with the laser efficiency measured in the core pumped single-clad CFW, in which all the pump and waveguide losses discussed previously can be significantly eliminated due to the much larger core size, the close to 100% pump absorption, and the much larger waveguide NA.

The waveguide propagating loss has been estimated in the 300 μm core waveguide, at a nonresonant wavelength of 632.8 nm. The transmitted laser power from the waveguide core is 88.2% of the total input power, corresponding to a maximum waveguide propagating loss coefficient of 0.013 cm^{-1}. In this Letter, we assume that the coupling efficiency of the input laser is 100% due to the larger waveguide core size and the NA, compared with the input laser beam. It is worth mentioning that the outer claddings for the current two waveguides consist of an infrared window grad ceramic spinel that has shown strong scattering loss, at both the laser and pump wavelengths. With future improvement on the quality of ceramic spinel or by using sapphire as outer claddings, the waveguide loss can be further reduced. The propagating loss in the double-clad waveguide is not measured in this experiment, since the coupling efficiency to the 40 μm waveguide core is unknown. However, the laser experimental results and the analyses presented previously suggest that it should have the comparable waveguide loss coefficient to the 300 μm core waveguide.

In conclusion, we have demonstrated the first LD cladding pumped single-mode laser in a double-clad Yb:YAG CFW, with near diffraction-limited beam quality. A laser output power of 13.2 W has been obtained at a pump power of 39.5 W. Our measurement and analysis indicate that the laser efficiency can be further increased, by improving the coupling and absorption efficiencies of the pump beam, as well as the NA and the end perpendicularity of the waveguide. The laser experiment has also demonstrated that single-mode lasing is achievable in multimode CFWs, when the waveguides only contain low-order modes. Potentially, the adhesive-free bonded CFWs can be used to improve the power scalability of current solid-state and fiber lasers.

This Letter was partially supported by NASA SBIR contract NNX13CG12P.

References

1. J. W. Dawson, M. J. Messerly, J. E. Heebner, P. H. Pax, A. K. Sridharan, A. L. Bullington, R. J. Beach, C. W. Siders, C. P. J. Barty, and M. Dubinskii, Proc. SPIE, **7686**, 768611 (2010).
2. J. L. Nightingale and R. L. Byer, Opt. Lett. **11**, 437 (1986).
3. P. C. W. Shi, I. A. Watson, and J. H. Sharp, Opt. Lett. **36**, 2182 (2011).
4. N. Soleimaril, B. Ponting, E. Gebremichael, A. Ribuot, and G. Maxwell, Proc. SPIE, **8959**, 895903 (2014).
5. Y. Zaouter, I. Martial, N. Aubry, J. Didierjean, C. Hönninger, E. Mottay, F. Druon, P. Georges, and F. Balembois, Opt. Lett. **36**, 748 (2011).
6. D. Sangla, N. Aubry, J. Didierjean, D. Perrodin, F. Balembois, K. Lebbou, A. Brenier, P. Georges, O. Tillement, and J.-M. Fourmigué, Appl. Phys. B **94**, 203 (2009).
7. X. Mu, H. Meissner, H.-C. Lee, and M. Dubinskii, Proc. SPIE **8237**, 82373M (2012).
8. N. Ter-Gabrielyan, V. Fromzel, X. Mu, H. Meissner, and M. Dubinskii, Opt. Lett. **38**, 2431 (2013).
9. I. J. Thomson, F. J. F. Monjardin, H. J. Baker, and D. R. Hall, IEEE J. Quantum Electron. **47**, 1336 (2011).
10. D. E. Zelmon, D. L. Small, and R. Page, Appl. Opt. **37**, 4933 (1998).
11. R. W. Waynant and M. N. Ediger, in *Electro-Optics Handbook*, 2nd ed. (McGraw-Hill, 2010), Chap. 11, p. 14.
12. H.-C. Lee, X. Mu, and H. Meissner, in *CLEO* (IEEE, 2011), paper AMB4.
13. R. C. Powell, *Physics of Solid-State Laser Materials*, Chapter 8 (Springer, 1998).
14. K. Okamoto, *Fundamentals of Optical Waveguides*, 2nd ed. (Academic, 2006).
15. K. S. Chiang, Opt. Quantum Electron. **17**, 381 (1985).
16. K. S. Chiang, Appl. Opt. **25**, 2169 (1986).
17. J. M. Khosrofian and B. A. Garetz, Appl. Opt. **22**, 3406 (1983).
18. J. P. Koplow, D. A. V. Kliner, and L. Goldberg, Opt. Lett. **25**, 442 (2000).
19. L. Goldberg, J. P. Koplow, and D. A. V. Kliner, Opt. Lett. **24**, 673 (1999).
20. P. Wang, L. J. Cooper, J. K. Sahu, and W. A. Clarkson, Opt. Lett. **31**, 226 (2006).
21. D. Marcuse, Bell Syst. Tech. J. **56**, 703 (1976).